American Mineralogist, Volume 92, pages 1593–1600, 2007

Vibrational dynamics in H^+-substituted forsterite: A first-principles molecular dynamics study

Dawn M. Shaw and John S. Tse*

Department of Physics and Engineering Physics, University of Saskatchewan, Saskatoon, Saskatchewan, S7N 5E2 Canada

Abstract

The vibrational spectra of H-substituted forsterite ($MgSiO_4H_2$) in which the Mg^{2+} at the M1 or M2 site is replaced by two H ions have been investigated by first-principles molecular dynamics calculations. Infrared spectra have been obtained and assigned with the aid of atomic vibrational density of states and the analysis of the atom radial distribution functions. It is shown that the proton dynamics are different at the M1 and M2 site. In the latter case, the proton does not remain bound to a single O atom but hops between O atoms in close proximity. This fluxional motion is highly temperature dependent. These fluxional motions results in substantially lower energy O-H stretching vibrations spanning a broad frequency range from 2000 to 3000 cm^{-1}. The present results will be useful for the characterization of the IR spectrum of H^+-substituted (leached) olivine under ambient conditions.

Keywords: Lattice dynamics, first-principles molecular dynamics, CPMD, olivine, forsterite, infrared spectroscopy

Introduction

There has been considerable interest in the structures and properties of minerals in the Earth's upper mantle. Of particular interest are those minerals containing water as bound hydroxyl (OH). These minerals are thought to be important to the formation of the Earth's oceans and atmosphere (Bell and Rossman 1992, and references therein). The presence of OH in the mineral structure may also help to explain the properties of the Earth's upper mantle. Although pyroxenes are thought to contribute the most to the water content of the upper mantle, a significant portion of the bound water is also found in the olivines. Recent XPS experiments on leached olivine indicated that H^+ ions could replace Mg^{2+} at the interface by as much as 10% (Zakanova-Herzog et al. in prep). Considering the significant contribution of hydrous olivines to the water content of the Earth's mantle, an understanding of the mechanism for water incorporation and the structure and dynamics of bound hydroxide in water-containing olivines is important in determining upper mantle properties. Although little is known about the mechanism, a recent combined experimental and theoretical study shows that protonation of O atoms bound to magnesium and the subsequent release of Mg^{2+} is the first step in the incorporation of water into forsterite (Liu et al. 2006). The exact mechanism of diffusion of the protons through the mineral, however, has not been clearly characterized.

Infrared (IR) spectroscopy is a valuable tool for the determination of the structure and concentration of hydroxide in a material. For natural and synthetic olivines, as well as forsterite, it has provided a wealth of information (Miller et al. 1987; McMillan et al. 1991; Bell and Rossman 1992; Wang et al. 1993; Kohlstedt et al. 1996; Kagi et al. 2000; Khisina and Wirth 2002; Demouchy and Mackwell 2003; Lemaire et al. 2004; Zhao et al. 2004; Asimow et al. 2006). Results of IR studies show that O-H stretch frequencies in Earth minerals normally cover the range from 2800 to 3700 cm^{-1} (Williams 1995). This is to be compared with the O-H stretching frequencies for molecules with covalent O-H bonds of 3400 to 3800 cm^{-1} (Harris and Bertolucci 1978). Thus, experimental results suggest that H^+ ion(s) incorporated into Earth minerals is (are) often strongly bound to the oxygen. However, the lower frequency range for an O-H stretch in minerals is not uncommon as the H atom may participate in H bonds with the surrounding O atoms. The stretching frequency is indicative of the strength of the O-H bond. The participation in H bonding is known to weaken this O-H bond slightly. Depending on the number and degree of H bonds as well as the structure and composition of the surroundings, the lowering of the corresponding vibrational frequency can be significant (Tsuchiya et al. 2005 and references therein). In some silicates present in the Earth's mantle, which contain OH groups, the IR spectra show a significant red shift on the order of 600 cm^{-1} (Libowitzky 1999). This observation suggests that the neighboring O atoms can have a significant influence on the O-H stretching vibration, and hence strongly affect the strength of the O-H bond. The central question is whether on average the H remains fixed to one O atom or hops between O atoms in the vicinity.

Recent theoretical studies (Brodholt 1997; Churakov et al. 2003; Tsuchiya et al. 2005) indicate that in some minerals there is more than one O site for binding with a H^+ ion. They also suggest that exchange of the proton between these sites can occur. Churakov et al. (2003) investigated possible structures for hydrous forsterite Hy-2a using static energy minimization. It was found that for each H^+ ion, substitution can occur at one

* E-mail: john.tse@usask.ca

of several O atoms close to the M1 and M2 sites. This study indicates the possibility that protons can be located over more than one position. However, only a limited number of possible structural models were suggested to occur in natural samples. Because pressure and temperature effects were not investigated, it is possible that the proton dynamics will be altered significantly by a substantial change in the pressure and/or temperature. This possibility has been suggested in another theoretical study showing that at high pressures the energy required for the exchange of a proton between two O atoms can be reduced (Tsuchiya et al. 2005). Thus, investigation of the dynamics of the protons may provide more insight into their behavior in H^+-substituted olivine both at ambient conditions and at higher temperatures and pressures. To the best of our knowledge, this effect has not been thoroughly investigated.

In this work, first-principles molecular dynamics calculations were employed to characterize the chemical bonding and vibrational dynamics of hydrous forsterite ($MgSiO_4H_2$). This work is motivated primarily by recent experiments using high-resolution X-ray photoelectron spectroscopy which show unequivocally that H^+ can replace Mg^{2+} in olivine upon hydration (Zakanova-Herzog et al. in prep; see also Liu et al. 2006). The results obtained here will be useful to guide the future assignment of the experimental IR spectrum for this system.

Naturally occurring olivine solid solution is comprised largely of forsterite (Mg_2SiO_4) component with a smaller amount of fayalite (Fe_2SiO_4), justifying the use of forsterite as a model for the study of the chemical bonding and dynamics of olivine. As will be shown below, it is found that (1) the dynamics of H substitution in the two nonequivalent metal sites (M1 and M2) are very different, and (2) at the M2 site, H atom is not confined to a single O site but fluctuates between several O atoms in the vicinity. First-principles molecular dynamics simulations performed at both 80 and 300 K provide a clear picture of the temperature effect on the proton dynamics. Since available experimental results have been obtained under ambient conditions, a comparison will be made with these results with the aim of obtaining a clear picture of proton dynamics at these conditions. Once this has been accomplished, further work will focus on pressure and temperature effects.

Computational details

Structural models

Ab initio (Car-Parrinello) molecular dynamics (CPMD 1990–2004) method within the density functional theory was used in this study. To check the consistency and accuracy of the numerical approach, initial geometry optimization on the pristine forsterite was also performed with the localized basis set program SIESTA (Soler et al. 2003). The Perdew-Burke-Enzerhof (PBE) exchange-correlation functional (Perdew et al. 1996) was used in the calculations. The effect of the core was treated using Troullier-Martins pseudopotentials (Troullier and Martins 1991). In the SIESTA method, a double-zeta plus polarization basis set with additional polarization functions was employed to describe the valence electrons. For the CPMD calculations, a plane wave basis set with an energy cutoff of 70 Rydberg was used. The Si, O, and H pseudopotentials were taken from the extended pseudopotential library of CPMD. For magnesium, a pseudopotential was constructed with the pseudopotential generation code fhi98PP (Fuchs and Scheffler 1999) using PBE functional. The cutoff radii for the *s* and *p* channels were set at 1.10 and 1.31 Å, respectively. The energy sampling was done for the Γ-point only (see below). Structural relaxations were performed using the preconditioned conjugate gradient method where convergence is achieved if the largest force on any nuclei is less than or equal to 0.0001 hartree/bohr.

A structural model for pristine forsterite was constructed from the known crystal structure of Mg_2SiO_4 (Bostrom 1987) with a space group *Pbnm* and unit-cell parameters $a = 4.749$, $b = 10.1985$, $c = 5.9792$ Å. The initial atom positions were taken from the American Mineralogist crystal structure database (Downs and Hall-Wallace 2003) and are given in Table 1. To test the accuracy of the method, atom positions with the simulation cell fixed to the experimental values were optimized using the localized basis set program SIESTA with a $2 \times 1 \times 2$ k-point set. The structure was also optimized with the pseudopotential plane wave program CPMD using only Γ-point sampling. The atom positions optimized with the two methods are compared with the positions obtained from experiment in Table 1. The relevant bond distances and angles are compared in Table 2. Both methods yield nearly identical results and compare very well with experiment. To evaluate effects of k-point sampling on the structure, the pristine forsterite was optimized using a $4 \times 2 \times 4$ k-point grid with the CPMD program. A comparison with the Γ-point results shows that little has changed in using a more extensive k-point grid. As a second test, two supercells ($2 \times 1 \times 2$ and $2 \times 2 \times 2$) were constructed. Again, the optimized structure is almost identical to the previous results (vide infra). We have also compared the calculated electronic density of states using localized basis set and plane wave basis set, and again found that the results are very similar. It was concluded that Γ-point sampling using the original cell (28 atoms) is adequate and therefore was employed in the ensuing calculations. It is noteworthy that the computational parameters employed here are very similar to previous theoretical studies on the structure of a hydrous olivine (Churakov et al. 2003) and proton dynamics in topaz-OH (Churakov and Wunder 2004), which have shown to provide highly satisfactory results.

Forsterite has two unique metal sites denoted as M1 and M2 (Bostrom 1987). Two hydrous $MgSiO_4H_2$ models were obtained by replacing a magnesium atom at each site by two protons. The resulting structures will be referred to as "structure 1" to denote substitution at M1 and "structure 2" to denote substitution at M2. The initial geometries for structures 1 and 2 were optimized with CPMD. As will be described in detail below, at finite temperature, the H^+ ions are found to be very mobile and neither hydrous $MgSiO_4H_2$ model adopts a bona fide "static" structure.

Molecular dynamics

The optimized geometries for structures 1 and 2 were used as starting models for molecular dynamics simulations (Tse 2002). The electronic ground state of the model systems were first quenched to the Born-Oppenheimer surface prior to molecular dynamics simulations. Molecular dynamics simulations were performed at 80 and 300 K using the Car-Parrinello (CP) dynamics for the electrons and classical dynamics for the nuclei in the micro-canonical (NVE) ensemble. A recent study involving the nature of proton dynamics in ice phase transitions has shown that at temperatures near 100 K, thermal effects dominate and quantum effects are of little importance to describe proton motions (Benoit et al. 1998). Since the temperatures in this work are near or above 100 K, it is expected that quantum effects will not greatly influence the proton motions, and are not considered (vide infra). The functionals, pseudopotentials, and energy sampling were identical to those used in the geometry optimizations. An electron mass of 800 a.u. was used in the CP fictitious dynamics of the electrons. The coupled electron and ion equations of motion were integrated with a time step of 0.12 femtoseconds (fs). For the systems studied here, thermodynamic equilibration was achieved in 1.8 picoseconds (ps). This was followed by 6 ps production runs where essential quantities (e.g., positions, velocity, dipole moments) were sampled every 1.2 fs and stored for later analysis. It was found that to maintain an average temperature of 300 K, a simple temperature correction scheme using velocity rescaling was adequate. However, for the 80 K simulations, this procedure was found to be insufficient. To control the temperature, a Nosé-Hoover chain (Nosé 1984; Hoover 1985) was applied to each ionic degree of freedom using a target temperature of 80 K and a characteristic frequency approximately equal to the highest frequency vibration in the mineral (manual, CPMD 1990–2004). Though the method of temperature control differs from that used for the pristine forsterite, this will not affect the spectra obtained as the use of the NVE ensemble with a carefully equilibrated system guarantees thermodynamic equilibrium.

Infrared spectra

Infrared (IR) intensities are related to the macroscopic electric polarization resulting from the radiation-induced vibrational motion of the system. This quantity is often defined as the total dipole moment of the unit cell. In a periodic system, the dipole moment is ill defined. In this case, the polarization cannot be represented by the cell's total dipole moment. The macroscopic polarization is instead obtained from the variation in the polarization between two states. An extensive review of

TABLE 1. Comparison of fractional coordinates of pristine forsterite

	Experiment			SIESTA			CPMD, Γ-point		
Atom	*x*	*y*	*z*	*x*	*y*	*z*	*x*	*y*	*z*
Mg1	0.0000	0.0000	0.0000	0.0000	0.0000	0.0000	0.0000	0.0000	0.0000
Mg2	0.9913	0.2773	0.2500	0.9933	0.2778	0.2500	0.9890	0.2771	0.2500
Si	0.4261	0.0940	0.2500	0.4277	0.0936	0.2500	0.4289	0.0990	0.2500
O1	0.7658	0.0919	0.2500	0.7693	0.0930	0.2500	0.7757	0.0947	0.2500
O2	**0.2210**	**0.4470**	**0.2500**	**0.2239**	**0.4463**	**0.2500**	**0.2175**	**0.4457**	**0.2500**
O3	**0.2774**	**0.1630**	**0.0329**	**0.2737**	**0.1630**	**0.0327**	**0.2657**	**0.1689**	**0.0276**

polarization in terms of the Berry phase has been described earlier (Resta 1994). If only the Γ-point was used in the simulation, the electronic dipole moment at time *t*, $M_\alpha^{el}(t)$ is obtained from the Berry phase,

$$M_\alpha^{el}(t) = \frac{2|e|}{G_\alpha(t)}\varphi\left[G_\alpha(t)\right] \quad (1)$$

where $G_\alpha(t)$ are the reciprocal lattice basis vectors, $\alpha = 1, 2, 3$, $\phi[G_\alpha(t)]$ represent the Berry phase

$$\varphi\left[G_\alpha(t)\right] = \mathrm{Im}[\ln \det S_{m,n}(t)] \quad (2)$$

and

$$S_{m,n}(t) = \left\langle \Phi_m(r,t) \middle| e^{-iG_\alpha(t)\cdot r(t)} \middle| \Phi_n(r,t) \right\rangle \quad (3)$$

is the overlap matrix.

The infrared spectra $I(\omega)$ were computed from the Fourier transform of the dipole autocorrelation function (McQuarrie 1976)

$$I_\alpha(\omega) = \frac{1}{2\pi}\int_{-\infty}^{\infty} dt e^{i\omega t}\left\langle M_\alpha(0)\cdot M_\alpha(t)\right\rangle \quad (4)$$

where $I(\omega)$ is the intensity at frequency ω and M_α is the total dipole moment (electronic and nuclear) of the system. IR active transitions in the calculated spectrum were examined by comparing with the vibrational density of states (VDOS) for individual atoms. The VDOS was obtained by a Fourier transform of the atom velocity self-autocorrelation function for each atom type in the structure. From the comparison, atomic contributions to the vibrations in an IR spectrum can be assigned.

Previous theoretical studies on kaolinite (Balan et al. 2001) and lizardite (Balan et al. 2002) have shown that the IR spectra of silicates in the region 400 to 4000 cm^{-1} were well reproduced using similar first-principles methods. It is anticipated that the spectra obtained here will also be of similar quality. In the far IR region, difficulties in the theoretical prediction of quantitative IR intensities are well known (Guillot 1991; Silvestrelli et al. 1997). To properly describe intensities in the IR spectrum, quantum corrections are required. Depending on the correction factor used, error in the IR peak intensity, however, can be as large as 60%. Comparison of calculated intensities is not always quantitative and the quality of the predicted IR spectra is determined here primarily by comparing the predicted and experimental peak positions.

RESULTS AND DISCUSSION

Structure and O-H, H-H bond distributions

Figures 1a and 1b show the O-H radial distribution functions (RDFs) for substitution at the M1 and M2 sites at 80 and 300 K, respectively. The first peak at ca. 1.05 Å, which is observed in all the O-H RDFs, corresponds to the covalent intramolecular O-H bond. It is clear from the figures that for O-H separations greater than 1 Å, the O-H RDFs at the M1 and M2 sites differ markedly at both 80 and 300 K.

For H^+-substitution at the M1 site at 80 K, the RDFs resemble an ordered crystalline solid with clear separations between the first two nearest neighbor coordination shells at 1.05 and 3.15 Å. Thus, at the M1 site, the H atoms participate only in a single O-H bond with an average O-H separation of 1.05 Å. The peaks in the RDF beyond 3 Å are not related to H bonding. It simply indicates the near-neighbor O···H separation. The RDF of the H^+-substituted (M1) olivine at 300 K is very similar to that at 80 K. The similarity shows that the dynamics of the protons have not changed substantially at the higher temperature. The peak centered at 3.15 Å, however, has broadened, indicating an increase in the thermal motions.

TABLE 2. Values of some representative bond lengths and angles in pristine forsterite

Parameter	Experiment	CPMD, Γ-point	CPMD, 4 × 2 × 4 grid
		Bond lengths (Å)	
Mg1-O1	2.09	2.07	2.07
Mg1-O2	2.09	2.07	2.07
Mg1-O3	2.13	2.14	2.14
Mg2-O1	2.17	2.12	2.12
Mg2-O2	2.05	2.03	2.03
Mg2-O3	2.07	2.05	2.05
Si1-O1	1.61	1.65	1.65
Si1-O2	1.65	1.71	1.71
Si1-O3	1.64	1.70	1.70
		Angles (°)	
O3-Mg1-O1	75.0	77.3	77.5
O3-Mg1-O2	95.0	97.3	97.2
O1-Mg1-O2	180.0	179.0	179.0
O3-Mg2-O3	88.7	87.4	87.4
O3-Mg2-O1	90.8	89.4	89.7
O1-Mg2-O1	177.3	176.3	176.0
O3-Si1-O3	105.0	103.3	103.0
O1-Si1-O2	**114.2**	**112.5**	**112.8**

In contrast, replacement of the magnesium atom at the M2 site with two H ions yields significantly different O-H RDFs from that at the M1 site. Substitution at the M2 site also yields a significantly different RDF at 300 K than at 80 K. At 300 K, apart from the intramolecular O-H bond at 1.05 Å, the RDFs show no clear sign of uniquely defined coordination shells for H^+ ions distributed around the O atoms. Instead, broad distributions of the O-H distance with maxima around 1.5, 2.4, and 3.0 Å are predicted. This observation suggests that the substitution of H^+ at the M2 site yields a structure with a high degree of dynamic disorder. On average, the protons can occupy several local minima in the vicinity of the substituted sites. At 80 K the peaks in the RDF are more clearly defined. The broad bands above ca. 1.4 Å are now split into several narrower bands. This indicates that at lower temperatures, the distribution of protons around the O atoms is somewhat localized with multiple local minima and therefore is dynamically slightly more ordered. The feature of the O-H RDF at 1.4 Å indicates that although the protons participate mainly in intramolecular O-H bonds (1.05 Å), there is a high probability that they also bridge the two nearest O atoms. At high temperature, disordering in the proton positions is obviously more significant and the protons spend more time exchanging between O atoms.

Figures 2a and 2b show the H-H RDF for the 80 and 300 K simulations, respectively. In both the 80 and 300 K simulations,

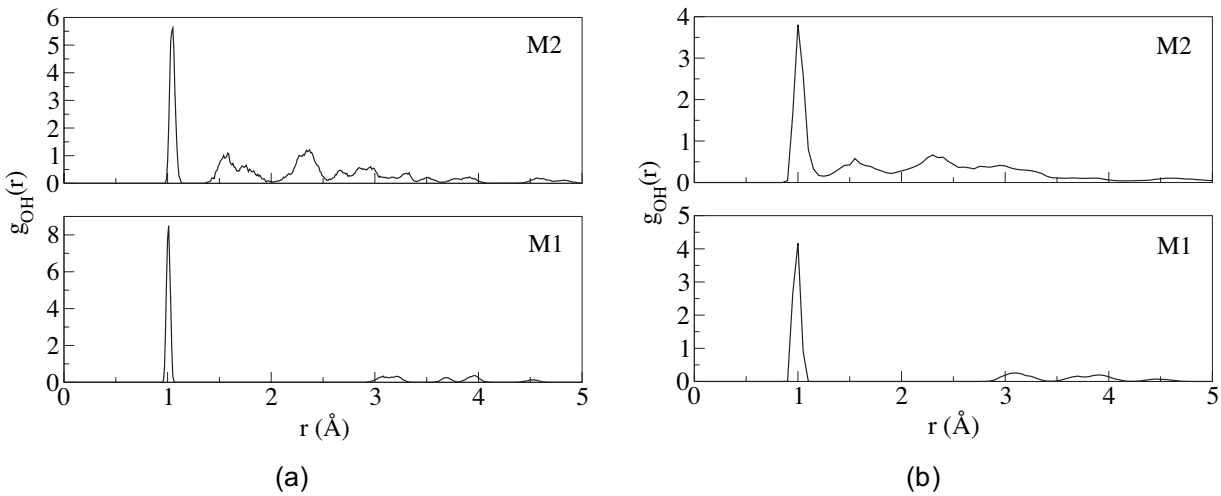

FIGURE 1. O-H radial distribution functions for $MgSiO_4H_2$ at (**a**) 80 K and (**b**) 300 K for proton substitution at the M1 and M2 site.

the average H···H separation is 2.3 Å. The large H···H distance indicates that at no time do the two protons approach each other. As shown in Table 3, the average H ion positions are quite close to the original magnesium M1 and M2 positions, showing that they remain localized within and are found at the vicinity of the empty Mg^{2+} sites. As expected, the H-H RDF at 300 K is broader than at 80 K. In both the 80 and 300 K simulations, substitution at the M2 site yields a broader H-H RDF. This indicates that there is a larger volume of free space sampled by the protons in the M2 site compared to the M1 site.

TABLE 3. Comparison of averaged proton positions with initial metal atom positions

Atom	*x*	*y*	*z*
Substitution at site M1			
Mg1	0.0000	0.0000	0.0000
$H_{ave,80K}$	–0.0299	0.0066	0.0369
$H_{ave,300K}$	–0.0139	–0.0215	–0.0194
Substitution at site M2			
Mg2	–0.0110	0.2771	0.2500
$H_{ave,80K}$	0.0337	0.2616	0.2405
$H_{ave,300K}$	0.0795	0.2502	0.2371

Infrared spectra

Before embarking on the discussion of the vibrational dynamics of hydrous olivines, the IR spectrum of pristine Mg_2SiO_4, where results from experiment are available for comparison, is examined in detail. Simulations of the IR spectra using Wannier functions were performed using the Γ-point only. A calculation with a more extensive k-point mesh would be too time-consuming. To check the validity of this simplification, the electronic density of states (DOS) calculated with a $4 \times 2 \times 4$ k-point set was compared to that computed using only the Γ-point. It was found that the DOS in both cases was similar, indicating that the electronic structure is not altered significantly by the addition of k-points in the calculation. Combining the observation presented earlier (vide infra) that the structural parameters are also almost identical, it is anticipated that the force constants, and thus the IR spectra, will not depend critically on the k-point grid. This suggestion is supported by a recent theoretical study of the IR spectrum of forsterite (Noel et al. 2006). The results presented here are expected to be of similar quality to a related study (Churakov et al. 2003), where a single k-point was also employed in the static structure calculations. Moreover, as will be shown below, the computed IR spectra and the polarization dependence are in good agreement with experimental results.

Figures 3a and 3b show calculated infrared spectra for Mg_2SiO_4 at 80 and 300 K, respectively. The vibrational density of states (VDOS) projected onto distinct atoms in the structure are also shown for comparison. Four peaks are clearly visible in the calculated IR spectra. These spectral features correspond nicely to those observed in the mid-infrared spectrum of forsterite (Wang et al. 1993). The two peaks at 800 to 1100 cm^{-1} and observed at 800 and 1050 cm^{-1} are attributed to Si and O motions. The peak above 1000 cm^{-1} is assigned to the Si-O stretching modes, while the band at around 860 cm^{-1} corresponds to the O-Si-O bending vibrations. The two IR active bands below 650 cm^{-1} show significant contributions from Mg, Si, and O from the VDOS. These bands are result of the coupling of stretching and bending modes of MgO_6 octahedra with the bending modes of SiO_4 tetrahedra. In accord with the theoretical prediction, the experimental IR spectrum also shows two bands at ca. 500 and 630 cm^{-1}. Below 400 cm^{-1}, all atoms contribute to the VDOS and the IR absorption can be assigned to translational motions of the crystal lattice.

Because forsterite has an orthorhombic space group, IR spectra of a single crystal at different crystal axes orientations provide information on the polarization dependence of the IR absorption. Figures 4a and 4b show the *x*, *y*, and *z* components of the far and mid-IR spectra for forsterite obtained from the 80 and 300 K MD simulations. Once again, the theoretical spectra are in substantial agreement with experimental polarized reflectance IR spectra (Hofmeister 1987) where 5 IR active bands were predicted and observed. The assignment of the peaks at 1000, 830, 550, and 450 cm^{-1} are the same as discussed above (supra infra). Vibrations between 200 and 300 cm^{-1} are due to the translational motion of magnesium atoms in the M1 and M2 sites. The IR bands below

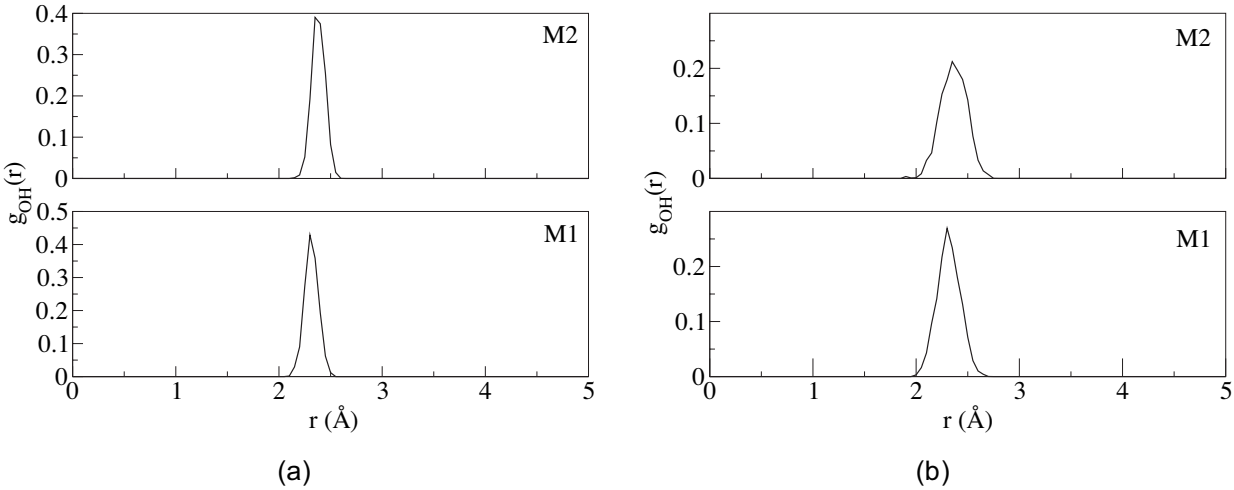

FIGURE 2. H-H radial distribution functions for $MgSiO_4H_2$ at (**a**) 80 K and (**b**) 300 K for proton substitution at the M1 and M2 site.

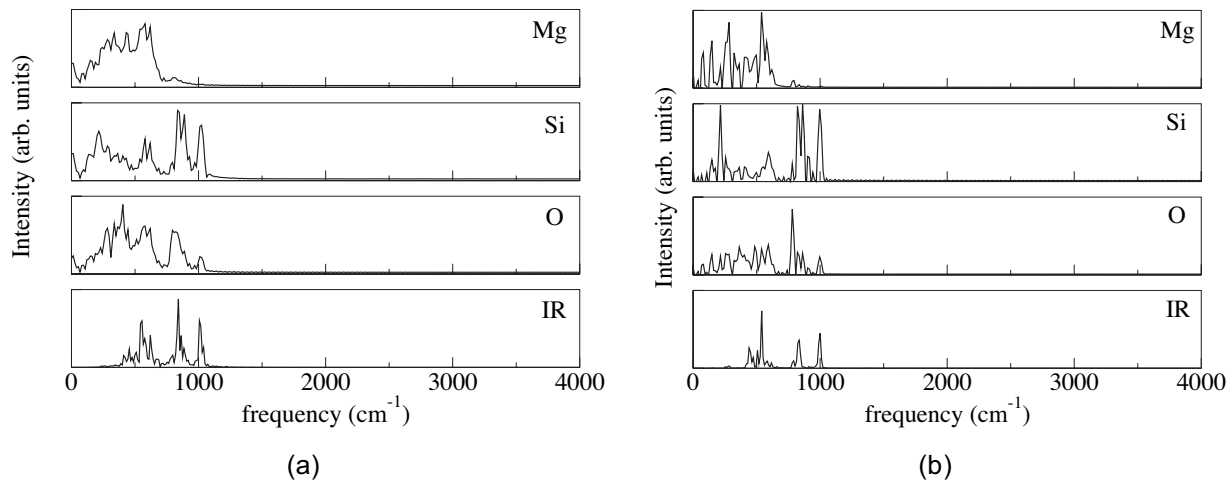

FIGURE 3. Calculated IR spectrum at (**a**) 80 K and (**b**) 300 K of pristine Mg_2SiO_4 and the VDOS for individual atoms.

200 cm^{-1} can be assigned to librations of the SiO_4 units. Since these two bands are relatively close to one another and are quite broad, it is likely that the band in the calculated spectrum is a combination of the magnesium translational motions in the M1 and M2 sites as well as librations of the SiO_4 units. Analysis of the VDOS supports this argument showing significant contributions from Mg in the region 300 to 400 cm^{-1} and large contributions from Si and O below 300 cm^{-1}.

Figures 5a and 5b show the calculated infrared spectra and VDOS at 80 and 300 K for a hydrous olivine with H^+-substitution at the M1 site. From the analysis of the projected atom VDOS, the assignments below 1000 cm^{-1} are similar to those given for Mg_2SiO_4 (see Figs. 3a and 3b). An exception is the presence of a larger number of peaks in H^+-substituted forsterite, which is likely the result of a lowering of the space group symmetry. The most significant differences in the M1 spectra between H^+-substituted and pristine forsterite occur in the region between 700 and 1200 cm^{-1} and around 2800 cm^{-1}. As indicated from the significant Si and O contributions to the VDOS, the peak at ca. 1000 cm^{-1} is assigned to the Si-O stretch. At 1100 cm^{-1}, there is a peak with large contributions from H, Si, and O atoms. Therefore, this peak likely originated from a Si-O-H bending mode. The two peaks between 700 and 900 cm^{-1} have large contributions from the Si and O VDOS and lie in a similar region to the assigned O-Si-O bend mode in the Mg_2SiO_4 spectrum. At 2840 cm^{-1}, there is a peak in the infrared spectrum with contributions almost solely from the protons. This peak is undoubtedly due to the O-H stretching modes but having a frequency lower than that observed in a free water molecule of 3400–3800 cm^{-1}. It is well known that as the O-H bond lengthens, its bond energy decreases resulting in a lowering of the stretching vibrational frequency. The O-H RDF for H^+ substitution at the M1 site shows a O-H bond distance of ~1.05 Å, which is longer than the 0.95 Å for a normal covalent O-H bond. A longer O-H distance in the H^+-substituted olivine is not surprising since the interaction of >O-H^+ is rather polar. Therefore, it is expected that the O-H vibrational frequency in

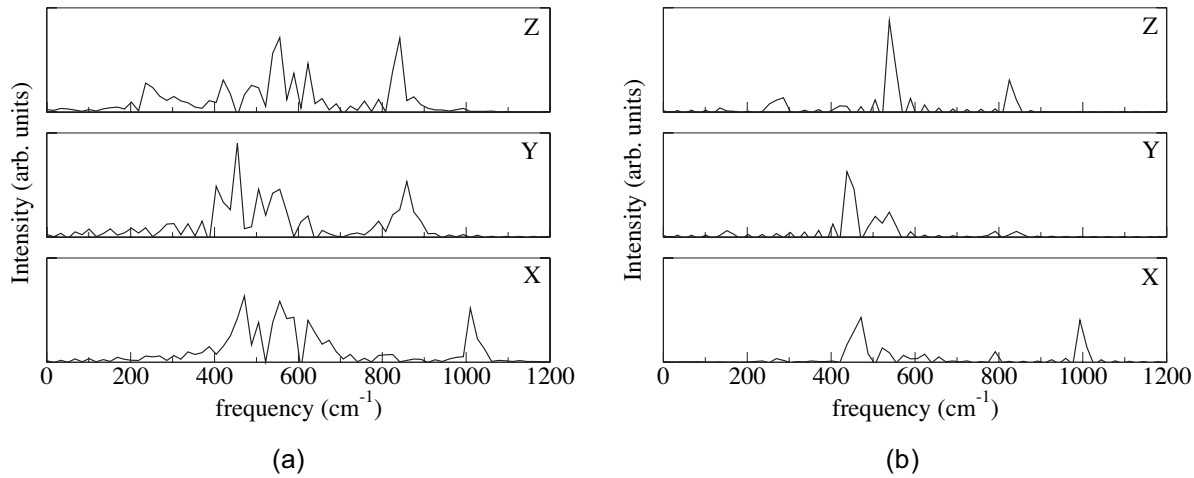

FIGURE 4. Calculated polarized IR spectrum for Mg_2SiO_4 at (**a**) 80 K and (**b**) 300 K.

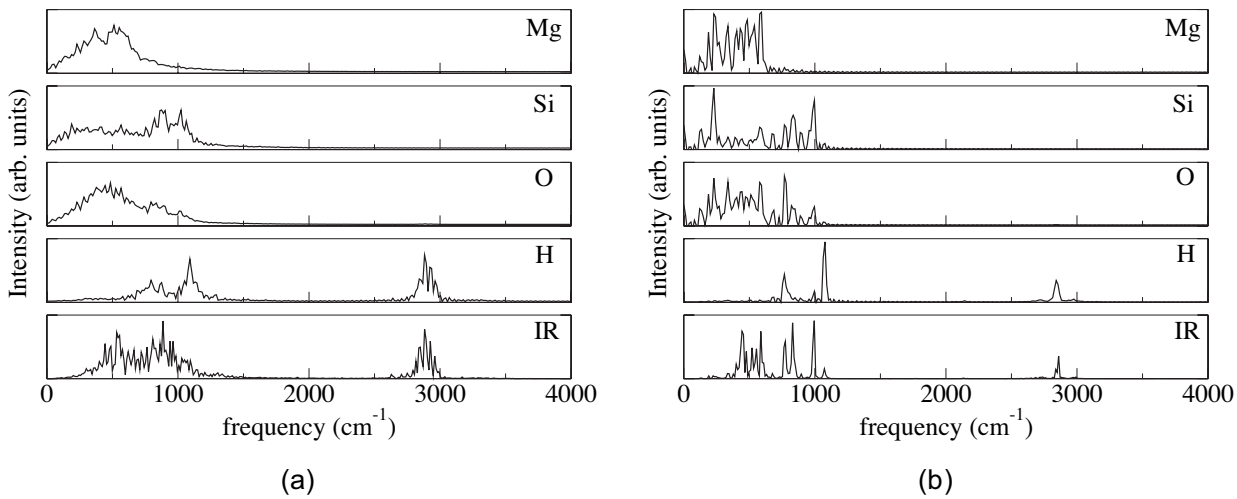

FIGURE 5. Calculated IR spectrum for $MgSiO_4H_2$ at (**a**) 80 K and (**b**) 300 K with H^+-substitution at the M1 site. The VDOS for individual atom types were also plotted for comparison.

H^+-substituted olivine should be lowered accordingly.

Figure 6a and 6b show calculated infrared spectra and VDOS for proton substitution at the M2 site at 80 and 300 K, respectively. These spectra differ substantially from that of proton substitution at the M1 site discussed above. Below 1000 cm^{-1}, the analysis parallels that for substitution at the M1 site except that additional peaks are predicted in the IR and VDOS for the H-substituted M2 site. These vibrations arise from the dynamical disorder and fluxional nature of the O-H interactions. It has been shown above that the protons sample a broad distribution of distances among the O atoms between 1.05 and 4.0 Å at the M2 site. This has a significant effect on the O-H stretching vibrational frequency. A previous study demonstrated that there is a correlation between the H bonding environment and the O-H stretching frequency (Emsley 1980). It was indicated that the O-H stretching frequency can vary between 1600 cm^{-1} in the case of strong H bonding to 3800 cm^{-1} in the case of weak H bonding. In this case the calculated O-H RDFs predicts a broad sampling of O-H distances, therefore, it is expected that the O-H stretches will cover a wider range in the IR spectrum. This is confirmed by the H VDOS, which shows significant participation in the vibration modes between 1900 and 3100 cm^{-1}. Because there are also significant H contributions to the bending vibrations between 800 and 1200 cm^{-1}, this may also explain the additional peaks that overlap with the SiO_4 tetrahedra stretching and bending modes.

Temperature effect on the proton dynamics at the M2 site

To illustrate the results derived from the analysis of the of calculated infrared spectra and RDFs for H^+-substitution at the M2 site, pictures depicting the temporal proton positions extracted from MD trajectories at 80 and 300 K are shown (Figs. 7a and 7b). In both cases, since the vibrational amplitudes for the Mg, Si, and O atoms are significantly smaller, the average positions over the entire 6 ps run are shown. The instantaneous positions of the protons are represented by white dots. The representation of the

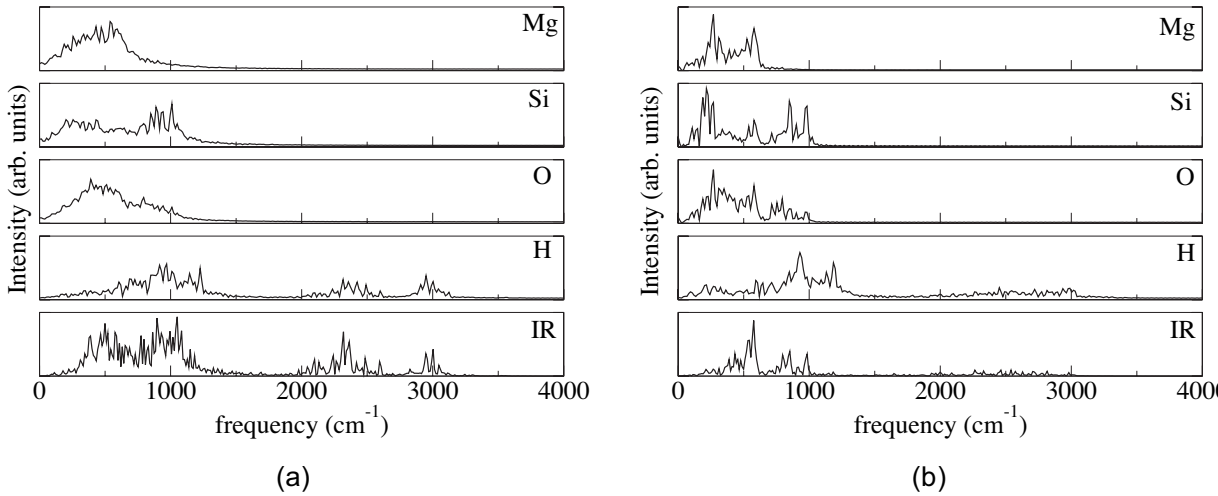

FIGURE 6. Calculated IR spectrum of $MgSiO_4H_2$ at (**a**) 80 K and (**b**) 300 K with H^+-substitution at the M2 site. The VDOS for individual atom types were also plotted for comparison.

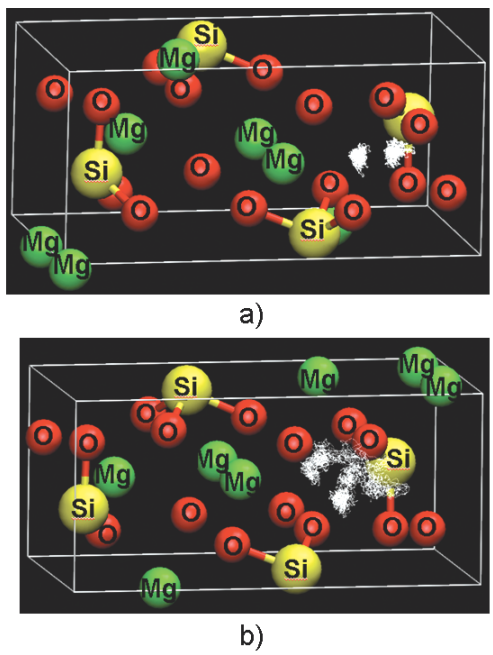

FIGURE 7. The trajectory of substituted protons at the M2 site in $MgSiO_4H_2$ from a 6 ps molecular dynamics simulation at (**a**) 80 K and (**b**) 300 K (see text for details).

proton positions in this manner shows approximately the volume of space they occupy. From Figure 7b, it can be seen vividly at 300 K that the H^+ ions do not localize in a small region of space as would be expected if they were bound to a single O atom. Instead, the protons migrate continuously between neighboring O atoms. This fluxional motion explains the broad distribution of O-H distances observed in the O-H RDF and the large number of peaks predicted in the IR and H VDOS. At 80 K, the volume of space that the protons can sample is smaller. This is reflected from the narrower distribution of O-H distances in the RDF and a smaller number of peaks in the IR and VDOS.

To evaluate the importance of quantum effects, the thermal wavelength,

$$\Lambda = \sqrt{\frac{h^2}{2\pi mkT}}$$

(where h is Planck's constant, m is the mass of the H atom, k is Boltzmann's constant, and T is the temperature) for an H at 80 and 300 K has been calculated. From statistical mechanics, quantum effects become important when the ratio $(V/N\Lambda^3) \leq 1$, where V is the cell volume and N is the number of particles in the cell (McQuarrie 1976). For an H atom at 300 K, the value of this ratio is 9.87. This value is much larger than 1 and so thermal effects should dominate, as expected. At 80 K, this ratio reduces to 1.36, which is still larger than 1. This indicates that even at 80 K the thermal effects are still important with small contributions from quantum effects. Thus classical dynamics may still be valid at 80K. Therefore, it is expected that the neglect of quantum effects will not adversely affect the dynamics of the protons at the temperatures employed in this study.

CONCLUDING REMARKS

Results of the present study demonstrate the importance of a dynamical picture of the proton delocalization effects in the IR spectra of olivine. To begin with, the results show that the theoretically calculated IR spectra of forsterite agree well with experiments. For hydrous olivines, spectral assignments require the explicit consideration of the fluxional proton dynamics illustrating the necessity of using first-principles molecular dynamics methods in the study of H in olivine systems. Furthermore, it is found that the dynamics of the protons in substituted forsterite depend on the Mg site. Protons in the M1 site are localized forming single covalent O-H bonds. In contrast, protons in the M2 site exchange rapidly with several neighboring O atoms as shown clearly in the broad distributions in the O-H RDF and VDOS. Consequently the IR spectrum for H^+-substitution at the M1 site shows only one peak at ca. 2900 cm^{-1}. This is indicative of a longer than normal intramolecular O-H bond. In contrast, IR spectra of H^+-substituted M2 site show the protons are not localized resulting in a larger number of IR peaks and shift to lower frequency between 2000 and 3000 cm^{-1}. At lower temperature, the protons are found to sample a narrower distribution of posi-

tions. Thus, the dynamics of the proton motion is very sensitive to the temperature.

More extensive theoretical studies under extreme conditions, such as those found in the Earth's mantle, are required to investigate the effects of temperature and pressure on the proton dynamics. Since mantle conditions are often difficult to reproduce in an experiment, theoretical calculations using state-of-the-art electronic methods can provide unique insight into the proton dynamics of H^+-substituted olivine. This will be the subject of a future study.

REFERENCES CITED

Asimow, P.D., Stein, L.C., Mosenfelder, J.L., and Rossman, G.R. (2006) Quantitative polarized infrared analysis of trace OH populations of randomly oriented mineral grains. American Mineralogist, 91, 278–284.

Balan, E., Saitta, A.M., Mauri, F., and Calas, G. (2001) First-principles modeling of the infrared spectrum of kaolinite. American Mineralogist, 86, 1321–1330.

Balan, E., Saitta, A.M., Mauri, F., Lemaire, C., and Guyot, F. (2002) First-principles calculation of the infrared spectrum of lizardite. American Mineralogist, 87, 1286–1290.

Bell, D.R. and Rossman, G.R. (1992) Water in the Earth's mantle: the role of nominally anhydrous minerals. Science, 255, 1391–1397.

Benoit, M., Marx, D., and Parrinello, M. (1998) Tunnelling and zero-point motion in high-pressure ice. Nature, 392, 258–261.

Bostrom, D. (1987) Single-crystal X-ray diffraction studies of synthetic Ni-Mg olivine solid solutions. American Mineralogist, 72, 965–972.

Brodholt, J. (1997) Ab initio calculations on point defects in forsterite (Mg_2SiO_4) and implications for diffusion and creep. American Mineralogist, 82, 1049–1053.

Churakov, S.V. and Wunder, B. (2004) Ab-initio calculations of the proton location in topaz-OH, $Al_2SiO_4(OH)_2$. Physics and Chemistry of Minerals, 31, 131–141.

Churakov, S.V., Khisina, N.R., Urusov, V.S., and Wirth, R. (2003) First-principles study of $(MgH_2SiO_4)\cdot n(Mg_2SiO_4)$ hydrous olivine structures. I. Crystal structure modeling of hydrous olivine Hy-2*a* $(MgH_2SiO_4)\cdot 3(Mg_2SiO_4)$. Physics and Chemistry of Minerals, 30, 1–11.

CPMD (1990–2004) Copyright IBM Corp., MPI für Festkörperforschung Stuttgart, 1997–2001.

Demouchy, S. and Mackwell, S. (2003) Water diffusion in synthetic iron-free forsterite. Physics and Chemistry of Minerals, 30, 486–494.

Downs, R.T. and Hall-Wallace, M. (2003) The American Mineralogist Crystal Structure Database. American Mineralogist, 88, 247–250.

Emsley, J. (1980) Very strong H bonding. Chemical Society Reviews, 9, 91–124.

Fuchs, M. and Scheffler, M. (1999) Ab initio pseudopotentials for electronic structure calculations of poly-atomic systems using density-functional theory. Computer Physics Communications, 119, 67–98.

Guillot, B. (1991) A molecular dynamics study of the far infrared spectrum of liquid water. Journal of Chemical Physics, 95, 1543–1551.

Harris, D.C. and Bertolucci, M.D. (1978) Symmetry and Spectroscopy an introduction to vibrational and electronic spectroscopy. Oxford University Press, New York.

Hofmeister, A.M. (1987) Single-crystal absorption and reflection infrared spectroscopy of forsterite and fayalite. Physics and Chemistry of Minerals, 14, 499–513.

Hoover, W.G. (1985) Canonical dynamics: Equilibrium phase-space distributions. Physical Review A, 31, 1695–1697.

Kagi, H., Parise, J.B., Cho, H., Rossman, G.R., and Loveday, J.S. (2000) H bonding interactions in phase A $[Mg_7Si_2O_8(OH)_6]$ at ambient and high pressure. Physics and Chemistry of Minerals, 27, 225–233.

Khisina, N.R. and Wirth, R. (2002) Hydrous olivine $(Mg_{1-y}Fe^{2+}_y)_{2-x}v_xSiO_4H_{2x}$—a new DHMS phase of variable composition observed as nanometer-sized precipitations in mantle olivine. Physics and Chemistry of Minerals, 29, 98–111.

Kohlstedt, D.L., Keppler, H., and Rubie, D.C. (1996) Solubility of water in the α, β, and γ phases of $(Mg, Fe)_2SiO_4$. Contributions to Mineralogy and Petrology, 123, 345–357.

Lemaire, C., Kohn, S.C., and Brooker, R.A. (2004) The effect of silica activity on the incorporation mechanisms of water in synthetic forsterite: A polarized infrared spectroscopic study. Contributions to Mineralogy and Petrology, 147, 48–57.

Libowitzky, E. (1999) Correlation of O-H stretching frequencies and O-H···O H bond lengths in minerals. Monatshefte für Chemie, 130, 1047–1059.

Liu, Y., Olsen, A.A., and Rimstidt, J.D. (2006) Mechanism for the dissolution of olivine series minerals in acidic solutions. American Mineralogist, 91, 455–458.

McMillan, P.F., Akaogi, M., Sato, R.K., Poe, B., and Foley, J. (1991) Hydroxyl groups in β-Mg_2SiO_4. American Mineralogist, 76, 354–360.

McQuarrie, D.A. (1976) Statistical Mechanics. Harper and Rowe Publishers, New York.

Miller, G.H., Rossman, G.R., and Harlow, G.E. (1987) The natural occurrence of hydroxide in olivine. Physics and Chemistry of Minerals, 14, 461–472.

Noel, Y., Catti, M., D'Arco, Ph., and Dovesi, R. (2006) The vibrational frequencies of forsterite Mg_2SiO_4: An all-electron ab initio study with the CRYSTAL code. Physics and Chemistry of Minerals, 33, 383–393.

Nosé, S. (1984) A unified formulation of the constant temperature molecular dynamics methods. Journal of Chemical Physics, 81, 511–519.

Perdew, J.P., Burke, K., and Ernzerhof, M. (1996) Generalized gradient approximation made simple. Physical Review Letters, 77, 3865–3868.

Resta, R. (1994) Macroscopic polarization in crystalline dielectrics: The geometric phase approach. Reviews of Modern Physics, 66, 899–915.

Silvestrelli, P.L., Bernasconi, M., and Parrinello, M. (1997) Ab initio infrared spectrum of liquid water. Chemical Physics Letters, 277, 478–482.

Soler, J.M., Artacho, E., Gale, J.D., García, A., Junquera, J., Ordejón, P., and Sánchez-Portal, D. (2003) The SIESTA method for ab initio order-N materials simulation. Journal of Physics: Condensed Matter, 14, 2745–2779.

Troullier, N. and Martins, J.L. (1991) Efficent pseudopotentials for plane-wave calculations. Physical Review B, 43, 1993–2006.

Tse, J.S. (2002) Ab initio molecular dynamics with density functional theory. Annual Review of Physical Chemistry, 53, 249–290.

Tsuchiya, J., Tsuchiya, T., and Tsuneyuki, S. (2005) First-principles study of H bond symmetrization of phase D under high pressure. American Mineralogist, 90, 44–49.

Wang, S.Y., Sharma, S.K., and Cooney, T.F. (1993) Micro-Raman and infrared spectral study of forsterite under high pressure. American Mineralogist, 78, 469–476.

Williams, Q. (1995) Infrared, Raman, and optical spectroscopy of Earth minerals. In T.J. Ahrens, Ed., Mineral Physics and Crystallography: A Handbook of Physical Constants, p. 291–302. AGU Reference Shelf 2, American Geophysical Union, Washington, D.C.

MANUSCRIPT RECEIVED AUGUST 25, 2006
MANUSCRIPT ACCEPTED JUNE 3, 2007
MANUSCRIPT HANDLED BY ARTEM OGANOV